

## Full paper

# Origin of achieving the enhanced activity and stability of Pt electrocatalysts with strong metal-support interactions via atomic layer deposition

Zhongxin Song<sup>a,1</sup>, Mohammad Norouzi Banis<sup>a,1</sup>, Lei Zhang<sup>a</sup>, Biqiong Wang<sup>a</sup>, Lijun Yang<sup>b</sup>, Dustin Banham<sup>b</sup>, Yang Zhao<sup>a</sup>, Jianneng Liang<sup>a</sup>, Matthew Zheng<sup>a</sup>, Ruying Li<sup>a</sup>, Siyu Ye<sup>b,\*</sup>, Xueliang Sun<sup>a,\*</sup>

<sup>a</sup> Department of Mechanical and Materials Engineering, University of Western Ontario, London, ON, Canada N6A 5B9

<sup>b</sup> Ballard Power Systems Inc., 9000 Glenlyon Parkway, Burnaby, BC, Canada V5J 5J8

## ARTICLE INFO

## Keywords:

Atomic layer deposition  
Electrocatalyst  
Oxygen reduction reaction  
Metal-support interaction

## ABSTRACT

The enhancement of catalyst activity and stability by controlling the metal-support interaction is significantly important for the long-term operation of polymer electrolyte membrane fuel cells (PEMFCs). In this work, an extremely stable electrocatalyst of platinum nanoparticles (Pt NPs) immobilized on a carbon support via the bridge layer of nitrogen-doped tantalum oxide (N-Ta<sub>2</sub>O<sub>5</sub>) is proposed. The novel N-Ta<sub>2</sub>O<sub>5</sub> bridge layer in between the Pt NPs and carbon surface is synthesized by an atomic layer deposition technique (ALD). It effectively prevents Pt nanocrystals from detachment, migration, and aggregation during the PEMFCs' operation. Electrochemical results indicate that the Pt/N-ALDTa<sub>2</sub>O<sub>5</sub>/C electrocatalyst exhibits superior durability and sufficient catalytic activity for the oxygen reduction reaction, compared to the Pt/C catalyst. X-ray absorption spectroscopy illustrates the strong interactions between the Pt NPs and the N-Ta<sub>2</sub>O<sub>5</sub>-decorated carbon support. It is found that the bridge layer of N-Ta<sub>2</sub>O<sub>5</sub> alters the electronic structure of the Pt nanocrystals and contributes to the significantly enhanced catalytic activity and durability for the Pt/N-ALDTa<sub>2</sub>O<sub>5</sub>/C catalyst. This strategy, by using ALD of N-doped metal oxide to tune the metal-support interface and results in strong metal-support interactions, will benefit the future design of new-generation electrocatalysts with even better activity and long-term durability for PEMFCs application.

## 1. Introduction

Due to the high efficiency in converting chemical energy from hydrogen into electrical energy, polymer electrolyte membrane fuel cell (PEMFCs) is considered as a promising technology among the renewable energy systems. Currently, PEMFCs are being commercialized for a broad range of applications, involving portable power, backup power and electric vehicles due to their high efficiency and zero emissions [1–3]. To realize a widespread commercial implementation of PEMFCs, developing a promising catalyst with enhanced oxygen reduction reaction (ORR) performance is of great significance. At present, carbon supported platinum nanoparticles (Pt NPs) are the state-of-the-art catalysts for ORR [4–7]. Dispersing Pt NPs on carbon increases the electrocatalytic activity and utilization of Pt, thus effectively decreasing the overall cost of PEMFCs. Carbon is used as a catalyst support material in PEMFCs due to its large surface area, high electrical conductivity, and well-developed pore structures [8–11]. However, the stability of Pt/C

for ORR cannot satisfy the requirement for long-term operation of PEMFCs. In addition to carbon corrosion at high potential during air-air startup/shutdown, the weak interactions between the carbon support and the metal particles lead to Pt NPs migration, aggregation, and eventually a degradation of electrocatalytic performance [12–14]. Numerous efforts have been devoted to solve this issue, for example, enhancing the interaction between Pt NPs and supports through carbon surface modification with metal compounds, polymers, etc. [15–22] or developing corrosion-resistant supports such as TiO<sub>2</sub> and ZrC [23–25]. It is reported the electrocatalysts exhibit improved stability and activity for the ORR by forming strong metal-support interactions (SMSIs). Utilization of SMSIs is a promising approach to improve both activity and stability of electrocatalysts. The SMSIs between Pt NPs and metal oxide supports have been investigated and have demonstrated positive effects on maintaining the stability of catalyst NPs [26,27]. However, the most stable metal oxides, with maximum valency, have poor electronic conductivity. This means the metal oxides as catalyst supports

\* Corresponding authors.

E-mail addresses: [siyu.ye@Ballard.com](mailto:siyu.ye@Ballard.com) (S. Ye), [xsun9@uwo.ca](mailto:xsun9@uwo.ca) (X. Sun).

<sup>1</sup> The first two authors contributed equally to this work.

<https://doi.org/10.1016/j.nanoen.2018.09.008>

Received 26 July 2018; Received in revised form 2 September 2018; Accepted 6 September 2018

Available online 07 September 2018

2211-2855/ © 2018 Elsevier Ltd. All rights reserved.

would enhance the catalysts' durability but sacrifice their high ORR activity. To enable the catalyst support with properties of both SMSIs and good electronic conductivity, one of the solutions is to develop metal oxide decorated carbon composites by combining the merits of metal oxide and carbon. Therefore, carbon decorated with highly dispersed metal oxide NPs could be used as alternative support for Pt catalyst [26–28]. By introducing metal oxide NPs to the position between the Pt NPs and the carbon support, the stable and strong three-phase boundary of Pt, metal oxide, and carbon could be achieved, which plays a significant role in stabilizing Pt NPs on the support. The group IV and V elements such as Zr, Ti, Ta, and Nb are known to be chemically stable under PEMFCs operation conditions. Several compounds based on these elements have been reported as ORR electrocatalysts or catalyst supports [29–33]. Despite many attempts, oxides based on Ta, Nb, and Zr have shown limited catalytic activity and durability for PEMFCs application due to their low conductivity. Based on these considerations, the nitrogen-doped support provides an opportunity to stabilize Pt NPs while indirectly improving the electrocatalytic activity due to stronger electronic interactions between Pt and a nitrogen-doped support. Nevertheless, using nitrogen-doped metal oxide as an additive to enable the Pt NPs catalyst with enhanced activity and long-term stability towards the ORR have not been reported.

Conventional synthesis methods for the group IV-V metal compounds have considerable disadvantages because the as-prepared particles are easily aggregated and frequently form large particles, making it difficult to precisely control the metal-support interface [34–36]. In contrast, the atomic layer deposition (ALD) technique has attracted considerable attention for the synthesis of transition metal oxide NPs on various substrates [37,38]. Due to the sequential reactions and self-limiting nature, ALD possesses the advantage in controlling the target materials with precise particle size and density on the substrate. By forming chemical bonds between the initial layer of ALD precursor and support atoms during the first cycle of deposition, the strong interaction between the deposited material and support can be enabled, which is believed beneficial for achieving the highly stable metal NPs [39]. Moreover, various transition metal oxides or compounds with controllable particle size and density have been developed on different substrates via ALD by our group [23,40–43]. These results enable the preparation of well-dispersed, nanoscale metal or metal oxide decorated on carbon surface, achieving the controllable metal-support interface.

Herein, we explored the role of nitrogen-doped tantalum oxide (N-Ta<sub>2</sub>O<sub>5</sub>) bridge layer in-between of Pt NPs and carbon support for a potential improvement in catalyst activity and durability by forming the SMSIs. Initially, the Ta<sub>2</sub>O<sub>5</sub> NPs were developed by ALD technique to decorate the carbon black surface. As co-support, Ta<sub>2</sub>O<sub>5</sub> NPs have much higher corrosion resistance in the electrochemical environment of PEMFCs compared to carbon. Subsequently, NH<sub>3</sub> treatment of ALDTa<sub>2</sub>O<sub>5</sub>/C support was conducted to doping N species, and resulted the N-doped-ALDTa<sub>2</sub>O<sub>5</sub>/C. It was found that Pt/N-ALDTa<sub>2</sub>O<sub>5</sub>/C catalyst showed enhanced catalytic activity and significantly improved electrochemical durability toward the ORR. X-ray absorption spectroscopy (XAS) indicated that the chemical states and electronic structure of Pt on N-ALDTa<sub>2</sub>O<sub>5</sub>/C support are mainly by a different appearance of higher unoccupied density of states of Pt 5d, which confirms strong interactions between Pt NPs and N-ALDTa<sub>2</sub>O<sub>5</sub>/C support. This is the first report for application of N-doped tantalum oxide as an effective stabilizer to immobilize the Pt NPs on carbon support. By tuning the metal-support interface, a highly active and stable Pt catalyst was achieved in this study.

## 2. Experiment

### 2.1. Surface modification of carbon black via ALD of tantalum oxide (Ta<sub>2</sub>O<sub>5</sub>)

Vulcan-72 carbon black was used as the catalyst support to prepare

the Pt/C catalyst. Prior to Pt deposition, surface modification of carbon black with Ta<sub>2</sub>O<sub>5</sub> NPs were carried out by an ALD technique. The Ta<sub>2</sub>O<sub>5</sub> deposition were conducted in an ALD reactor (Savannah 100, Cambridge Nanotechnology Inc., USA) at 225 °C using tantalum (V) ethoxide (Ta(OC<sub>2</sub>H<sub>5</sub>)<sub>5</sub>) and H<sub>2</sub>O as precursors, and N<sub>2</sub> as carrier gas. One ALD cycle consisted of the following six steps: (1) 0.5 s pulse of Ta(OC<sub>2</sub>H<sub>5</sub>)<sub>5</sub>; (2) 3.0 s extended exposure to Ta(OC<sub>2</sub>H<sub>5</sub>)<sub>5</sub> in the reaction chamber; (3) N<sub>2</sub> purging of 16 s; (4) 1.0 s pulse of H<sub>2</sub>O; (5) 3.0 s extended exposure to H<sub>2</sub>O in the reaction chamber; (6) N<sub>2</sub> purging of 25 s. 35 ALD cycles were carried out to achieve a uniform distribution of Ta<sub>2</sub>O<sub>5</sub> NPs on carbon surface. The prepared sample is designated as ALDTa<sub>2</sub>O<sub>5</sub>/C. More detailed relationships between ALD cycles and Ta<sub>2</sub>O<sub>5</sub> loading have been previously reported elsewhere [8,41]. To investigate the impact of N-doped-metal oxide on Pt catalyst activity and durability, the N-doped ALDTa<sub>2</sub>O<sub>5</sub>/C (N-ALDTa<sub>2</sub>O<sub>5</sub>/C) was derived from post-treatment of ALDTa<sub>2</sub>O<sub>5</sub>/C with NH<sub>3</sub>/Ar (10:100) under 700 °C for 1 h. The modified N-ALDTa<sub>2</sub>O<sub>5</sub>/C and ALDTa<sub>2</sub>O<sub>5</sub>/C composites were supplied as supports for Pt NPs deposition and finally the supported Pt/N-ALDTa<sub>2</sub>O<sub>5</sub>/C and Pt/ALDTa<sub>2</sub>O<sub>5</sub>/C catalysts were prepared respectively. To investigate whether N can be doped in carbon, one sample of NH<sub>3</sub>-treated-carbon (NH<sub>3</sub>/C) with NH<sub>3</sub>/Ar (10/100) post-treating carbon under 700 °C for 1 h was designed.

### 2.2. Pt deposition on nanocomposite carbon supports

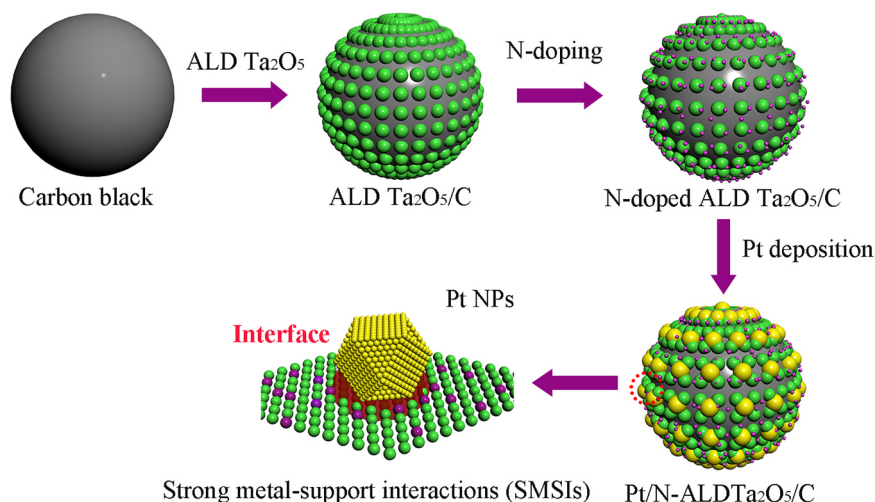
For Pt deposition, a microwave assisted ethylene glycol (EG) reduction method was used to deposit Pt NPs on different supports. The 20 mg of N-ALDTa<sub>2</sub>O<sub>5</sub>/C in 50 ml EG solution containing 0.6 mM H<sub>2</sub>PtCl<sub>6</sub>·6H<sub>2</sub>O was sonicated for 30 min, and then saturated NaOH/EG solution was used to adjust the pH of the solution to ~10. The solution mixture was microwaved in an oven until the boiling point of EG was reached. During the microwaving process, Pt metallic NPs nucleation and growth proceeded by reducing the H<sub>2</sub>PtCl<sub>6</sub> precursor. The Pt NPs were then loaded on the available substrate surface of the N-ALDTa<sub>2</sub>O<sub>5</sub>/C support. After cooling down, filtering, and washing, the obtained Pt/N-ALDTa<sub>2</sub>O<sub>5</sub>/C catalyst was dried in a vacuum oven. For comparison, the Pt NPs were also deposited on the ALDTa<sub>2</sub>O<sub>5</sub>/C and pure Vulcan-72 carbon supports using the same procedure to get the Pt/ALDTa<sub>2</sub>O<sub>5</sub> and Pt/C catalysts, respectively.

### 2.3. Physical characterization

Structure characterizations of ALDTa<sub>2</sub>O<sub>5</sub>/C, N-ALDTa<sub>2</sub>O<sub>5</sub>/C and Pt/N-ALDTa<sub>2</sub>O<sub>5</sub>/C catalysts were performed by high resolution transmission electron microscope (HRTEM, JEOL 2010FEG, at 200 kV). The elemental distribution was determined by energy dispersive X-ray spectroscopy (EDS) and electron energy loss spectroscopy (EELS) mapping. The chemical state of N-ALDTa<sub>2</sub>O<sub>5</sub>/C, and NH<sub>3</sub>/C were investigated by X-ray photoelectron spectroscopy (XPS, Kratos Axis Ultra-spectrometer). The XPS demonstrated that N content was around 0.5 at %, and Ta content around 3.3 at% (equal to 12.7 wt% determined by EDS) for the sample of N-ALDTa<sub>2</sub>O<sub>5</sub>/C. Pt content for each of the electrocatalysts was determined by inductively coupled plasma-optical emission spectroscopy (ICP-OES). From ICP analysis, the Pt loading in Pt/N-ALDTa<sub>2</sub>O<sub>5</sub>/C, Pt/ALDTa<sub>2</sub>O<sub>5</sub>/C, and Pt/C catalysts were determined to be 21.0 wt%, 22.6 wt%, and 23.7 wt%, respectively.

### 2.4. X-ray absorption spectroscopy

X-ray absorption near edge structure (XANES) measurements at the Pt L<sub>3</sub>-edge (11,564 eV) and L<sub>2</sub>-edge (13,273 eV) were performed on the 061D superconducting wiggler sourced hard X-ray microanalysis (HXMA) beamline at the Canadian Light Source. The spectra were collected in fluorescence yield mode using a 32 Ge solid-state detector, and the spectra of high purity metal Pt foil were collected in transmission mode for comparison and mono energy calibration. The



**Scheme 1.** Schematic illustration for fabrication of nanocomposite electrocatalyst of Pt/N-ALDTa<sub>2</sub>O<sub>5</sub>/C with strong metal-support interactions (SMSIs).

acquired XANES data were processed according to the standard procedures using the Athena module. The XANES oscillation functions were obtained by subtracting the pre-edge and post-edge background from the overall absorption spectra and then normalized with respect to the edge-jump step to unity. For a better understanding of the impact of unoccupied densities of 5d states of Pt NPs on different supports, quantitative whiteness (WL) intensity analysis were conducted based on the method reported by Mansour et al. [44], Sham et al. [45,46], and Sun et al. [17,47,48]. The details that support the quantitative WL intensity analysis are available in the [Supporting information](#).

### 2.5. Electrochemical characterization

The electrochemical characterizations were performed in a three-electrode system using a rotating-disk electrode (RDE) setup with an Autolab electrochemistry station and rotation control (Pine Instruments). The ink was prepared by mixing 3.0 mg of catalyst in 3.0 ml of aqueous solution containing 0.6 ml of isopropyl alcohol and 30  $\mu$ l of Nafion (5.0 wt%). Then 30 min sonication was conducted to ensure homogenous dispersion and wetting of the catalyst. 20  $\mu$ l of the catalyst ink was pipetted onto a polished glassy carbon electrode (Pine, 5.0 mm dia., 0.196 cm<sup>2</sup>) and allowed to dry at room temperature. All electrochemical measurements were carried out in 0.1 M HClO<sub>4</sub> electrolyte using a Pt wire as a counter electrode and reversible hydrogen electrode (RHE) as a reference electrode. All potentials reported henceforth are vs. RHE. Each electrode was activated by scanning from 0.05 to 1.1 V at 50 mV s<sup>-1</sup> in N<sub>2</sub>-saturated 0.1 M HClO<sub>4</sub> until no changes were observed in the cyclic voltammetry (CV) curves. O<sub>2</sub> was bubbled into HClO<sub>4</sub> for 30 min to achieve an O<sub>2</sub>-saturated electrolyte. Then, ORR linear sweep voltammetry (LSV, 10 mV s<sup>-1</sup>) was conducted in O<sub>2</sub>-saturated 0.1 M HClO<sub>4</sub> on the RDE system with a rotation speed of 1600 rpm. The LSV curves obtained under N<sub>2</sub> were subtracted from the LSV curves obtained under O<sub>2</sub> to remove the non-Faradaic current. The electrochemically active surface area (ECSA) was calculated by integrating the area of the CV curves in the hydrogen underpotential deposition (HUPD) region and using the charge value of 210  $\mu$ C cm<sup>-2</sup> corresponding to a monolayer adsorption of hydrogen atoms on a polycrystalline Pt catalyst [49]. To evaluate the catalysts durability, an accelerated durability test (ADT) of potential cycling from 0.6 to 1.0 V vs. RHE protocol was conducted on the as-prepared electrocatalysts. A total of 10,000 cycles in O<sub>2</sub>-saturated 0.1 M HClO<sub>4</sub> at 50 mV s<sup>-1</sup> were performed to analyze the catalysts' durability. Intermediate characterizations were recorded to monitor the catalysts' ECSA degradation and mass activity loss.

### 3. Results and discussion

The nanocomposite electrocatalyst with Pt NPs supported on N-ALDTa<sub>2</sub>O<sub>5</sub>/C was synthesized by a three-step procedure as illustrated in [Scheme 1](#). Initially, ALD of Ta<sub>2</sub>O<sub>5</sub> NPs were performed on the surface of carbon black to produce the Ta<sub>2</sub>O<sub>5</sub>-modified carbon. Based on our previous work [8], 35 ALD cycles can ensure appropriate loading and uniform distribution of Ta<sub>2</sub>O<sub>5</sub> NPs on the carbon surface. Thus, 35 ALD cycles were adopted here for the Ta<sub>2</sub>O<sub>5</sub> NPs deposition. The gas mixture of ammonia/argon (NH<sub>3</sub>/Ar = 10/90) was used for the post-treatment of ALDTa<sub>2</sub>O<sub>5</sub>/C support under 700 °C for 1 h to achieve the N-doped ALDTa<sub>2</sub>O<sub>5</sub>/C nanocomposite support. By doping the N atoms from NH<sub>3</sub> to Ta<sub>2</sub>O<sub>5</sub> NPs, the composite of ALDTa<sub>2</sub>O<sub>5</sub>/C can be transformed into N-Ta<sub>2</sub>O<sub>5</sub>/C support. Finally, the Pt NPs were deposited on the surface of the N-Ta<sub>2</sub>O<sub>5</sub>/C support with a controlled Pt loading of ~20 wt% to obtain the nanocomposite electrocatalyst of Pt/N-ALDTa<sub>2</sub>O<sub>5</sub>/C.

The particle sizes and distribution of ALDTa<sub>2</sub>O<sub>5</sub> NPs on carbon spheres achieved via ALD was characterized by HRTEM and scanning transmission electron microscopy (STEM). It can be observed in [Fig. 1\(a, b\)](#) that the Ta<sub>2</sub>O<sub>5</sub> NPs with discontinuous morphology were deposited on the carbon surface with a uniform distribution. By further analysis HRTEM information, no crystal lattice stripe can be found which implies that the majority of Ta<sub>2</sub>O<sub>5</sub> NPs present as amorphous state [41], that is due to the small particles size (2.7  $\pm$  0.3 nm) of Ta<sub>2</sub>O<sub>5</sub> and the low temperature (225 °C) of ALD synthesis mechanism. To understand the structure and morphology variations for ALDTa<sub>2</sub>O<sub>5</sub>/C after N-doping, a comparison of HRTEM/STEM images for N-ALDTa<sub>2</sub>O<sub>5</sub>/C was conducted. [Fig. 1c](#) and [d](#) indicate that the N-Ta<sub>2</sub>O<sub>5</sub> from support of N-ALDTa<sub>2</sub>O<sub>5</sub>/C has similar particle size with that of Ta<sub>2</sub>O<sub>5</sub>, which exhibits uniform dispersion across the Vulcan carbon surface. Although having undergone a high temperature NH<sub>3</sub> treatment (700 °C), the N-Ta<sub>2</sub>O<sub>5</sub> NPs still retained a good dispersion and were closely anchored on the carbon surface, suggesting a tight integration of N-Ta<sub>2</sub>O<sub>5</sub> NPs and carbon surface. To further confirm the N species have successfully doped into the ALDTa<sub>2</sub>O<sub>5</sub>/C, EELS element maps were conducted, and showed uniform distribution of N atoms in the N-ALDTa<sub>2</sub>O<sub>5</sub>/C support ([Fig. 1e](#)). Using N-ALDTa<sub>2</sub>O<sub>5</sub>/C as a catalyst support, Pt NPs were deposited on this nanocomposite support, and finally, the supported Pt/N-ALDTa<sub>2</sub>O<sub>5</sub>/C electrocatalyst was achieved. The HRTEM image in [Fig. 1f](#) shows that crystalline Pt NPs were uniformly dispersed on N-ALDTa<sub>2</sub>O<sub>5</sub>/C support. No Pt NPs aggregation was detected. The pre-deposited N-Ta<sub>2</sub>O<sub>5</sub> appears as an island surrounding the Pt NPs on the carbon surface, effectively preventing the Pt NPs migration and aggregation with the neighbouring NPs. This characterization is evidence of stabilization against mobility that the N-Ta<sub>2</sub>O<sub>5</sub>

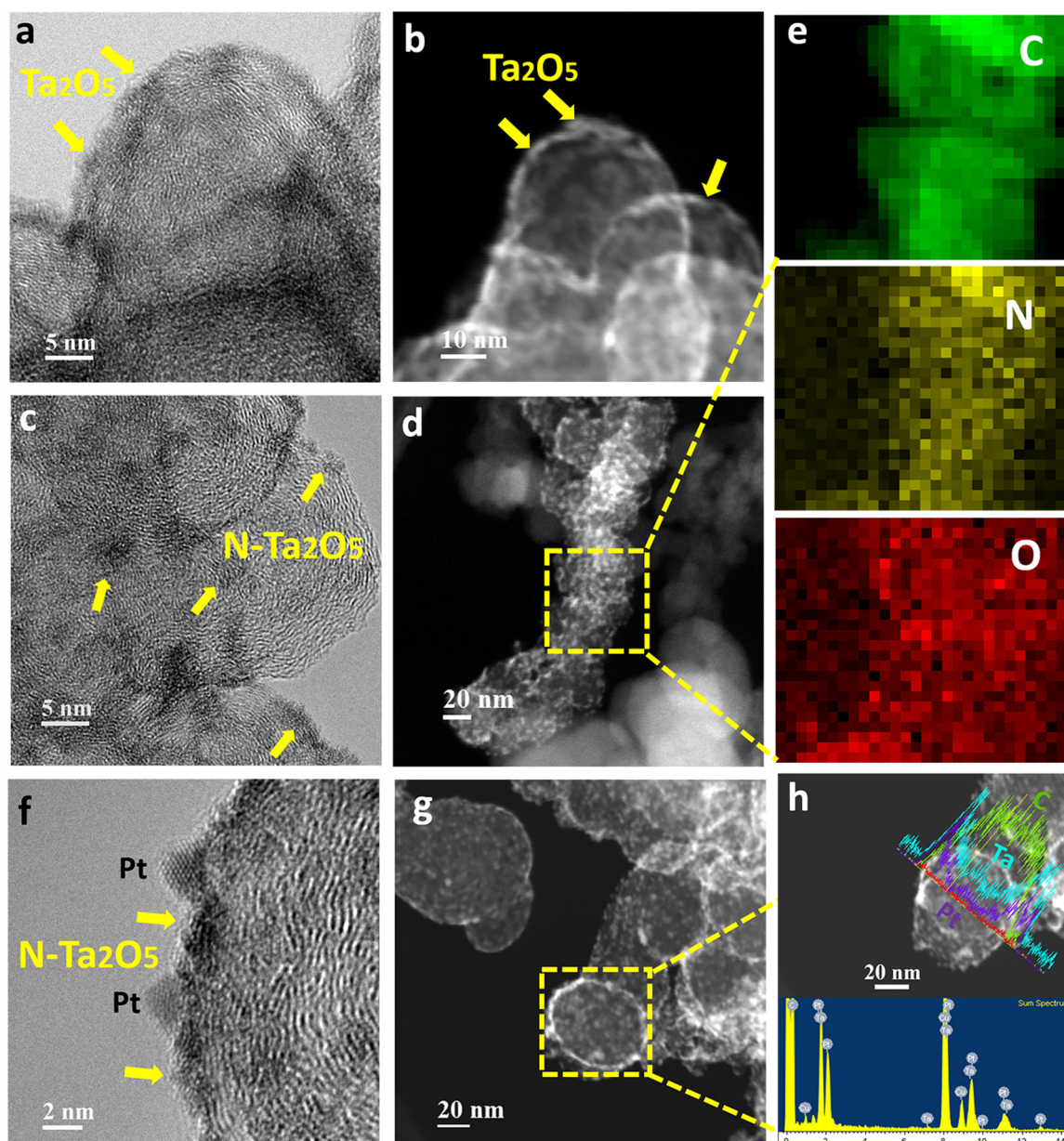


**Fig. 1.** HRTEM and STEM images of ALDTa<sub>2</sub>O<sub>5</sub>/C (a-b), N-ALDTa<sub>2</sub>O<sub>5</sub>/C (c-d), and Pt/N-ALDTa<sub>2</sub>O<sub>5</sub>/C (f-g); EELS map of the C (green), N (yellow), O (red) elements for the N-ALDTa<sub>2</sub>O<sub>5</sub>/C (e); STEM-EDS line scan and spectra of Pt/N-ALDTa<sub>2</sub>O<sub>5</sub>/C (h).

bridge particle imparts on the Pt NPs. The HRTEM/EDS mapping (Fig. S1) shows Pt and Ta with uniform distribution on a carbon surface. STEM line scan images in Fig. 1g and h provide convincing evidence for the effective incorporation of Pt with N-Ta<sub>2</sub>O<sub>5</sub> NPs and carbon support. EDS spectra indicates the Ta and Pt loading is 12.7 wt% and 20.1 wt%, respectively, which is consistent to the Pt content of 21.0 wt% detected by ICP-OES. By tuning the interface between Pt NPs and carbon support via the bridge layer of N-ALDTa<sub>2</sub>O<sub>5</sub> NPs, the Pt/N-ALDTa<sub>2</sub>O<sub>5</sub>/C electrocatalyst is expected to have enhanced electrocatalytic activity and stability compared to pure Pt/C.

A smaller particle size with a higher specific surface area in the current work is believed to provide a higher thermodynamically metastable surface area to facilitate the nitridation reaction, thereby yielding the N-doped Ta<sub>2</sub>O<sub>5</sub> in addition to Ta<sub>2</sub>O<sub>5</sub>. Nitrogen doping of ALDTa<sub>2</sub>O<sub>5</sub>/C via the 700 °C NH<sub>3</sub> treatment was confirmed by X-ray photoelectron spectroscopy (XPS), which was carried out to determine the chemical composition of N-ALDTa<sub>2</sub>O<sub>5</sub>/C. The XPS survey of N-ALDTa<sub>2</sub>O<sub>5</sub>/C in Fig. 2a indicates the presence of Ta, O, N and C

elements with the atomic content of 3.3%, 9.2%, 0.5% and 87.0%, respectively. The Ta 4f doublets in Fig. 2b, with binding energy of 27.09 eV for the Ta f<sub>7/2</sub> peak and 28.97 eV for the Ta f<sub>5/2</sub> peak, are consistent with the Ta<sup>5+</sup> signal from Ta<sub>2</sub>O<sub>5</sub>. The XPS spectra in Fig. 2c showed N1s peak at 397.7 eV accompanied with a larger Ta 4p<sub>3/2</sub> peak at 405.1 eV. This confirms that nitrogen atoms have been successfully doped into the Ta<sub>2</sub>O<sub>5</sub> lattice. As reported by Kang et.al [50], the nitrogen-doping content in Ta<sub>2</sub>O<sub>5</sub> can be modulated by the temperature of NH<sub>3</sub> treatment. Under 700 °C, certain amounts of O atoms from Ta<sub>2</sub>O<sub>5</sub>/C are substituted by N atoms with larger radii than that of O atoms. Fig. 2d indicates that major O1s peak located at 531.6 eV is from the metal oxide of Ta<sub>2</sub>O<sub>5</sub>, and a small peak at 533.2 eV is attributed to the response of O-N, belonging to the N-doped-O species from N-ALDTa<sub>2</sub>O<sub>5</sub>/C. In this study, the O/Ta molar ratio is 2.78 and the N/Ta molar ratio was 0.15, which suggest that nitrogen atoms have been doped in a modest concentration via the 700 °C NH<sub>3</sub> treatment for 1 h. To understand the N is actually doped in Ta<sub>2</sub>O<sub>5</sub> NPs or both Ta<sub>2</sub>O<sub>5</sub> and carbon surface. The NH<sub>3</sub>-treated-carbon (NH<sub>3</sub>/C) material was

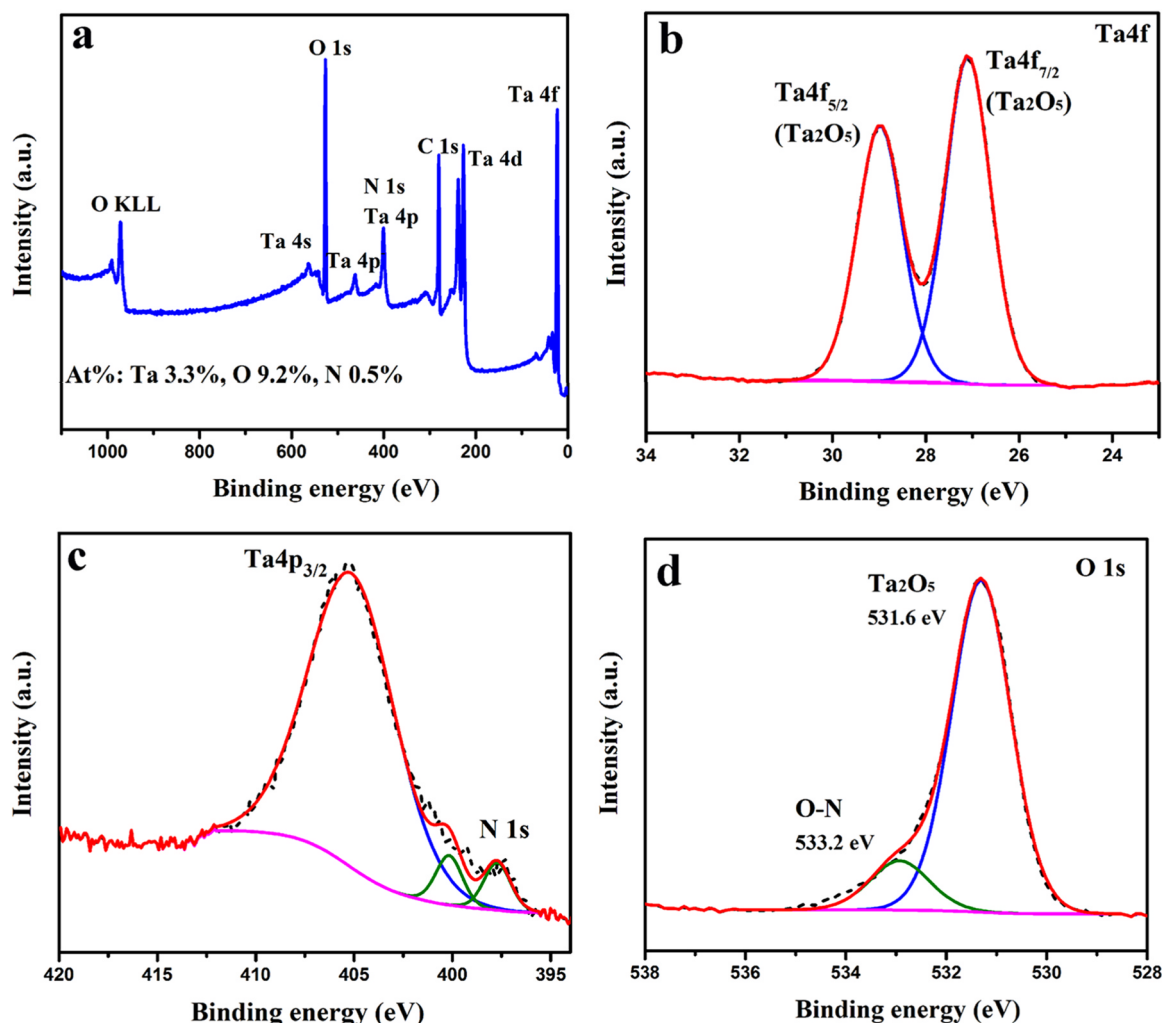


Fig. 2. X-ray photoelectron spectra for N-ALDTa<sub>2</sub>O<sub>5</sub>/C nanocomposite. a) survey spectrum, b) Ta 4f<sub>5/2</sub> and Ta 4f<sub>7/2</sub>, c) Ta 4p<sub>3/2</sub> and N 1s, and d) O 1s.

prepared by treatment of carbon with NH<sub>3</sub>/Ar at 700 °C. From the XPS spectra (Fig. S2), it can be found that quite low O levels (0.8%) and no N signal is detectable in the sample of NH<sub>3</sub>/C, suggesting the very inert carbon surface and no N atoms can be doped in the carbon under 700 °C heat treatment. Therefore, it is believed that in the system of N-ALDTa<sub>2</sub>O<sub>5</sub>/C sample, all the N atoms are doped in the Ta<sub>2</sub>O<sub>5</sub> NPs.

To determine the impact of N-ALDTa<sub>2</sub>O<sub>5</sub> and ALDTa<sub>2</sub>O<sub>5</sub> on Pt activity and durability, the ORR activity and potential cycling durability for catalysts of Pt/N-ALDTa<sub>2</sub>O<sub>5</sub>/C, Pt/ALDTa<sub>2</sub>O<sub>5</sub>/C, and Pt/C were evaluated. The durability tests were performed by potential cycling between 0.6 V and 1.0 V (vs. RHE) in O<sub>2</sub>-purged 0.1 M HClO<sub>4</sub> for 10,000 cycles to mimic catalyst durability under the PEMFCs operation. During the accelerated durability test (ADT), Pt catalysts underwent the NPs migration and aggregation, dissolution, and re-deposition, thus reducing active surface area, leading to activity degradation. Fig. S3 illustrates the representative CV curves (Fig. S3 a-c) recorded before and after 10,000 cycles ADT for these catalysts. The electrochemical active surface area (ECSA) and relationships between ECSAs and cycle numbers for each catalyst are shown in Table S1 and Fig. S3d, respectively. With continuous potential cycling, the CV curves for Pt/C catalyst exhibited a pronounced decrease of total charge in the hydrogen underpotential deposition (HUPD) region, indicating a degradation in Pt active surface area. By analyzing the ECSA of the Pt/C catalyst before and after 10,000 cycles ADT, it was observed that the Pt/C catalyst experienced a significant surface degradation, with 47% initial ECSA loss after cycling. In contrast, the Pt/ALDTa<sub>2</sub>O<sub>5</sub>/C catalyst, with the

decoration of ALDTa<sub>2</sub>O<sub>5</sub> NPs on carbon surface, exhibited an enhanced stable CV peak current and showed 25.2% loss of ECSA after ADT-10,000. The more stable ECSA for Pt/ALDTa<sub>2</sub>O<sub>5</sub>/C than that of Pt/C implies an adhesive and/or anchoring effect of T<sub>2</sub>O<sub>5</sub> bridge particles, which benefits for immobilizing Pt NPs and inhibiting Pt NPs migration and aggregation, thus alleviating the rapid degradation of catalyst surface area. More importantly, with further doping N species into the ALDTa<sub>2</sub>O<sub>5</sub>, N-ALDTa<sub>2</sub>O<sub>5</sub> NPs display the best effectiveness in stabilizing Pt NPs. Fig. S3 (a) shows the CV curves for Pt/N-ALDTa<sub>2</sub>O<sub>5</sub>/C catalyst before and after ADT-10,000. Higher beginning ECSA of 70.3 m<sup>2</sup> g<sub>Pt</sub><sup>-1</sup> and 85.1% initial ECSA was maintained, only 14.9% ECSA loss was revealed for the Pt/N-ALDTa<sub>2</sub>O<sub>5</sub>/C catalyst, after 10,000 cycles ADT. These results suggest a superior durability of Pt/N-ALDTa<sub>2</sub>O<sub>5</sub>/C compared to the Pt/ALDTa<sub>2</sub>O<sub>5</sub>/C and Pt/C catalysts.

The ORR kinetics of these Pt electrocatalysts were evaluated by comparing their polarization curves that were acquired in O<sub>2</sub>-saturated 0.1 M HClO<sub>4</sub> (Fig. 3a-c) and the calculated mass activities based on Koutecky-Levich plots (Fig. 3d) [51]. After performing 10,000 cycles ADT, the Pt/C lost their ORR activity much faster than that of the Pt/ALDTa<sub>2</sub>O<sub>5</sub>/C and Pt/N-ALDTa<sub>2</sub>O<sub>5</sub>/C catalysts, i.e., a pronounced 20 mV (shifted from 0.891 V to 0.871 V) of half-wave potential (E<sub>1/2</sub>) degradation for Pt/C versus 10 mV (shifted from 0.902 to 0.892 V) E<sub>1/2</sub> degradation for Pt/ALDTa<sub>2</sub>O<sub>5</sub>/C. In contrast, the E<sub>1/2</sub> of Pt/N-ALDTa<sub>2</sub>O<sub>5</sub>/C electrocatalyst remained almost the same as their respective voltammograms nearly overlapped and only 4 mV of E<sub>1/2</sub> (shifted from 0.908 to 0.904 V) loss was observed before and after the

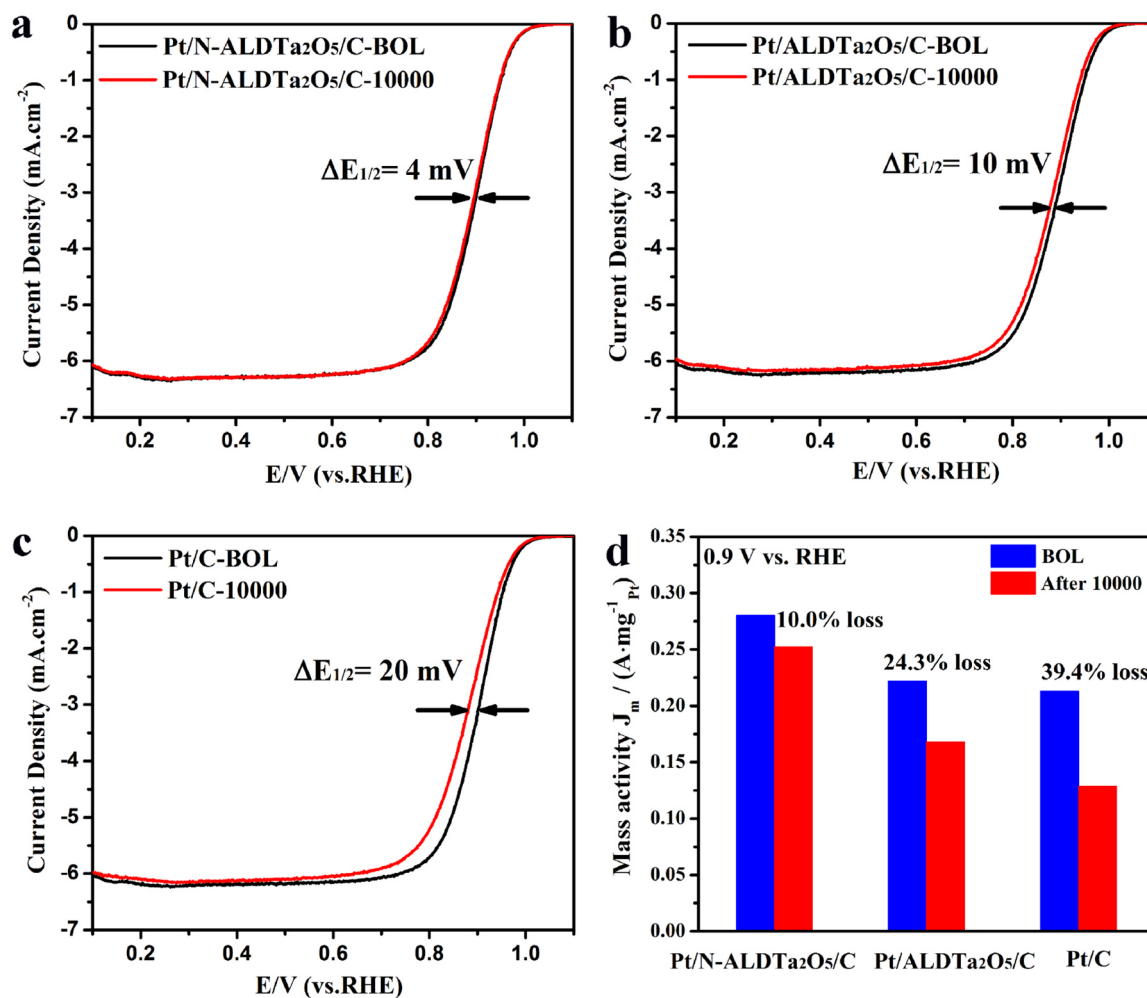


**Fig. 3.** polarization curves of (a) Pt/N-ALDTa<sub>2</sub>O<sub>5</sub>/C, (b) Pt/ALDTa<sub>2</sub>O<sub>5</sub>/C, and (c) Pt/C before and after 10,000 cycles of accelerated durability tests (ADT) in O<sub>2</sub>-saturated 0.1 M HClO<sub>4</sub>, 1600 rpm, scan rate of 10 mV s<sup>-1</sup>. (d) mass activity of different catalysts at 0.9 V (vs. RHE) before and after ADT-10,000 (BOL stands for beginning of life).

stability test. The kinetic currents at 0.9 V for all the studied electrocatalysts obtained from the Koutecký-Levich equation [51] were used to get Pt mass activities (Fig. 3d). With the same Pt NPs size and loading, the electrocatalyst of Pt/N-ALDTa<sub>2</sub>O<sub>5</sub>/C showed the best mass activity and durability. The mass activity of Pt/C exhibited obvious degradation of 39.4% activity loss after 10,000 cycles ADT. Pt/ALDTa<sub>2</sub>O<sub>5</sub>/C electrocatalyst showed an initial mass activity of 0.222 A·mg<sub>Pt</sub><sup>-1</sup>, and after 10,000 ADT cycles, the mass activity decreased to 0.168 A·mg<sub>Pt</sub><sup>-1</sup>, showing a 24.3% loss. Notably, Pt/N-ALDTa<sub>2</sub>O<sub>5</sub>/C showed a higher initial activity of 0.280 A·mg<sub>Pt</sub><sup>-1</sup>. After 10,000 ADT cycles, its mass activity decreased to 0.252 A·mg<sub>Pt</sub><sup>-1</sup> (with only 10.0% loss in Pt activity) that is higher than the initial mass activity of Pt/C, and around 2 times better than that for Pt/C after 10,000 ADT cycles (detailed mass activity and E<sub>1/2</sub> numbers for each catalyst are list in Table S1). The ORR and potential cycling durability tests show that the Pt/N-ALDTa<sub>2</sub>O<sub>5</sub>/C electrocatalyst processes the enhanced ORR activity and stability than that of Pt/ALDTa<sub>2</sub>O<sub>5</sub>/C and Pt/C catalysts. The morphology change of the Pt/N-ALDTa<sub>2</sub>O<sub>5</sub>/C catalyst after 10,000 cycles ADT was examined by TEM. As shown in Fig. S4, after ADT, the size of the Pt NPs in Pt/N-ALDTa<sub>2</sub>O<sub>5</sub>/C was 3.3 nm and underwent almost no change, suggesting that the effective anchoring of N-ALDTa<sub>2</sub>O<sub>5</sub> bridge layer in stabilizing Pt NPs during potential cycling. These results indicate a superior durability of Pt/N-ALDTa<sub>2</sub>O<sub>5</sub>/C compared to the Pt/ALDTa<sub>2</sub>O<sub>5</sub>/C, and Pt/C catalysts. The enhanced durability is ascribed to the strong metal-support interactions between Pt NPs and N-ALDTa<sub>2</sub>O<sub>5</sub>/C support, which

hinder the migration and agglomeration of Pt NPs during electrochemical operation, consequently preserving the high intrinsic activity. In addition, the strong Pt-support interactions alters the electronic structures of Pt atoms, which promotes the Pt NPs with enhanced activity than the pristine Pt/C catalyst. To confirm this assumption, the X-ray absorption spectroscopy was carried out to study the local electronic structures of Pt and evaluate the metal-support interactions in these electrocatalysts.

To determine the chemical state and electronic structure of Pt and Pt-support interactions, the X-ray absorption spectra of Pt at L<sub>3</sub>- and L<sub>2</sub>-edge were studied. It is seen that the X-ray absorption near edge structure (XANES) of supported Pt NPs at both the Pt L<sub>3</sub>- and the L<sub>2</sub>-edge exhibit a considerable whiteline (WL) compared to the Pt foil (Fig. 4). The WL at Pt L<sub>2</sub> and L<sub>3</sub> edges arise from the dominant 2p<sub>1/2</sub> and 2p<sub>3/2</sub> transition to 5d<sub>3/2</sub> and 5d<sub>5/2,3/2</sub>, respectively, indicating the presence of unoccupied densities of states (DOS) of Pt 5d<sub>5/2</sub> and 5d<sub>3/2</sub> characters in the catalysts. The unoccupied DOS are crucial to the catalytic performance of Pt catalyst [47]. The normalized XANES and derivative spectra for both the Pt L<sub>3</sub>- and L<sub>2</sub>-edges of the Pt/N-ALDTa<sub>2</sub>O<sub>5</sub>/C, Pt/ALDTa<sub>2</sub>O<sub>5</sub>/C, and Pt/C catalysts are shown in Fig. 4, in comparison to a standard Pt foil. It can be observed in Fig. 4a that the threshold energy (E<sub>0</sub>) and the maximum energy (E<sub>peak</sub>) of the Pt L<sub>3</sub>-edge for these supported Pt catalysts are close to the reference of metallic Pt foil, confirming the metallic nature of the Pt NPs. However, the XANES profile and derivative spectra of Pt in the Pt/N-ALDTa<sub>2</sub>O<sub>5</sub>/C catalyst

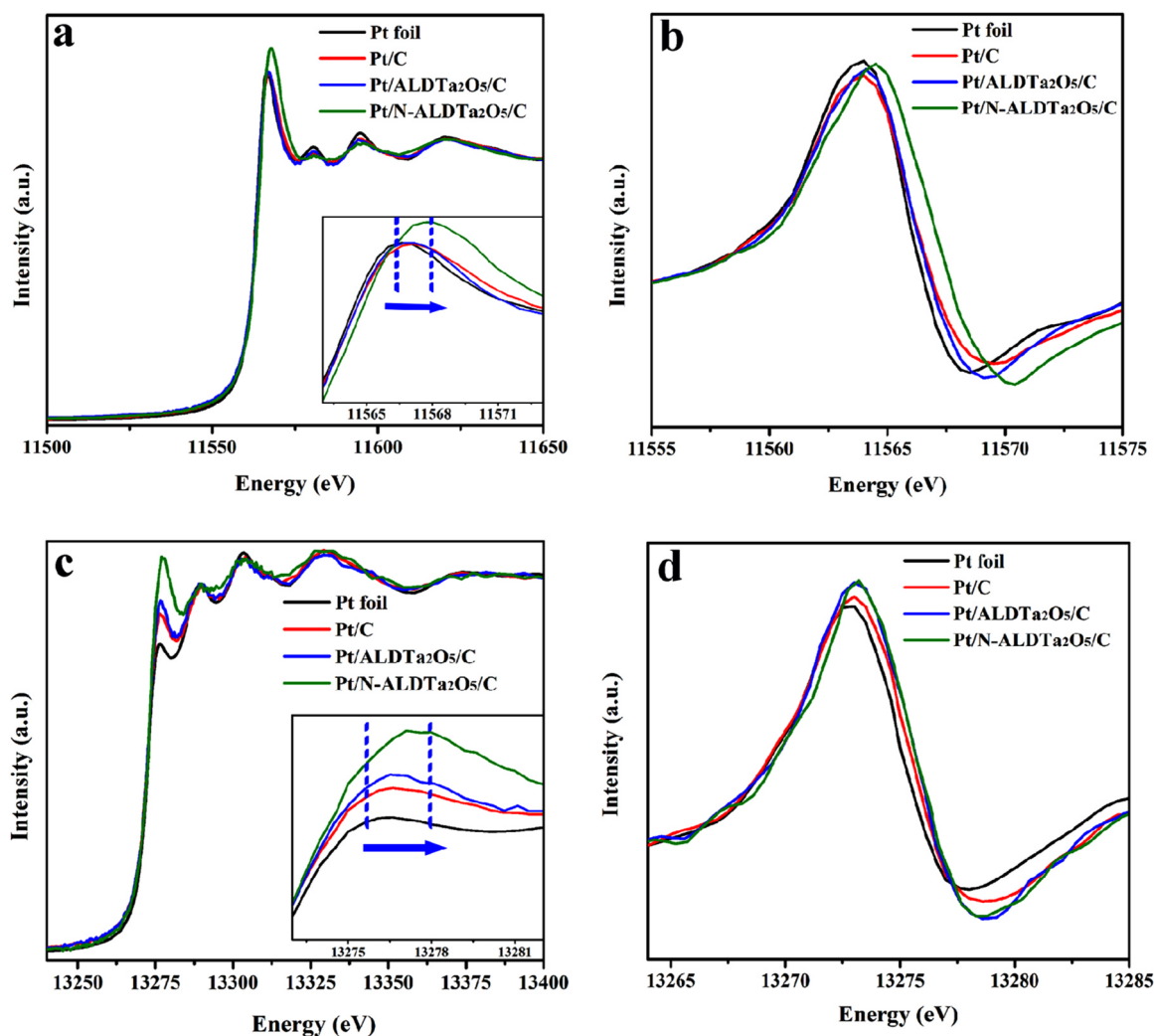


**Fig. 4.** X-ray absorption studies. (a) The normalized and (b) derivative XANES spectra at the Pt  $L_3$ -edge of the Pt/N-ALDTa<sub>2</sub>O<sub>5</sub>/C, Pt/ALDTa<sub>2</sub>O<sub>5</sub>/C, Pt/C and Pt foil. The inset shows the enlarged spectra at the Pt  $L_3$ -edge white line (WL). (c) The normalized and (d) derivative XANES spectra at the Pt  $L_2$ -edge of Pt/N-ALDTa<sub>2</sub>O<sub>5</sub>/C, Pt/ALDTa<sub>2</sub>O<sub>5</sub>/C, Pt/C and Pt foil. The inset shows the enlarged spectra at the Pt  $L_2$ -edge white line (WL).

demonstrate a dramatic difference from those of the Pt/ALDTa<sub>2</sub>O<sub>5</sub>/C and Pt/C catalysts. The higher WL intensity (Fig. 4a) and the positively shifted peak energy in derivative spectra (Fig. 4b) for Pt/N-ALDTa<sub>2</sub>O<sub>5</sub>/C, compared to other catalysts, implies that the depletion of the Pt d-band in Pt/N-ALDTa<sub>2</sub>O<sub>5</sub>/C is greater than that of Pt/ALDTa<sub>2</sub>O<sub>5</sub>/C and Pt/C catalysts. The appearance of higher unoccupied density of d states of Pt is due to the electron transfer from Pt to N-Ta<sub>2</sub>O<sub>5</sub> NPs, which confirms the strong interactions between Pt NPs and N-Ta<sub>2</sub>O<sub>5</sub>/C

support. Moreover, the corresponding Pt  $L_2$ -edge WL exhibits considerable variation among the catalysts. These results indicate that  $L_2$ -edge WL intensity increases in the order of: Pt foil < Pt/C < Pt/ALDTa<sub>2</sub>O<sub>5</sub>/C < Pt/N-ALDTa<sub>2</sub>O<sub>5</sub>/C, which follows the same order with the long-term durability of these catalysts. Therefore, the increase of the WL intensity in Pt/N-ALDTa<sub>2</sub>O<sub>5</sub>/C compared to Pt/ALDTa<sub>2</sub>O<sub>5</sub>/C and Pt/C, reflects strong interaction between the Pt and the N-Ta<sub>2</sub>O<sub>5</sub>/C support. The quantitative analysis to determine the occupancy of 5d

**Table 1**

Pt  $L_3$ -edge and Pt  $L_2$ -edge threshold and whiteline parameters of different catalysts.

Sample	Pt $L_3$ edge WL				Pt $L_2$ edge WL						
	$E_0$ (eV) <sup>a</sup>	$E_{(peak)}$ (eV) <sup>b</sup>	$\Gamma$ (eV) <sup>c</sup>	$\Delta A_3$ <sup>d</sup>	$E_0$ (eV) <sup>a</sup>	$E_{(peak)}$ (eV) <sup>b</sup>	$\Gamma$ (eV) <sup>c</sup>	$\Delta A_2$ <sup>d</sup>	$h_{5/2}$	$h_{3/2}$	Total
Pt Foil	11,564	11,566.6	4.0	6.173	13,273	13,276.4	2.5	2.516	0.572	0.117	0.689
Pt/C	11,564	11,567.1	5.4	6.776	13,273	13,276.6	1.9	3.753	0.620	0.175	0.795
Pt/ALDTa <sub>2</sub> O <sub>5</sub> /C	11,563.9	11,566.9	4.5	7.018	13,273	13,276.8	1.3	3.956	0.642	0.184	0.826
Pt/N-ALDTa <sub>2</sub> O <sub>5</sub> /C	11,564.5	11,567.8	5.9	7.388	13,273	13,277.6	5.1	4.203	0.676	0.196	0.871

<sup>a</sup> Position of the point of inflection of the rising edge.

<sup>b</sup> Peak position.

<sup>c</sup> Line width at Half maximum of the WL.

<sup>d</sup> Area under the difference curve for unity edge jump, the unity edge jump for the Pt  $L_3$  and  $L_2$  edge corresponds to a value of  $2.5 \times 10^3 \text{ cm}^{-1}$  and  $1.16 \times 10^3 \text{ cm}^{-1}$ , respectively.

states through detailed examination of WL profile in each sample will be further discussed below.

For a better understanding of the effect of the unoccupied densities of 5d states of Pt on different supports, the quantitative analysis of Pt L<sub>3</sub> and L<sub>2</sub> edge WL intensity was conducted based on the method (see details in [Supporting information](#)) reported by Sham et al. [45] and Sun et al. [17,47] For the set of experimental data recorded in this work, the Pt L<sub>3</sub> and L<sub>2</sub> edge threshold, WL parameters, and the corresponding 5d hole counts of h<sub>3/2</sub> and h<sub>5/2</sub> are summarized in [Table 1](#). These results quantitatively confirm the observations made on the Pt L<sub>3</sub> and L<sub>2</sub> edge XANES: the Pt/N-ALDTa<sub>2</sub>O<sub>5</sub>/C has the highest total unoccupied DOS of the 5d hole counts of 0.871, higher than that of 0.826 for Pt/ALDTa<sub>2</sub>O<sub>5</sub>/C and 0.795 for Pt/C. The character of Pt 5d unoccupied density of states correlates well with its performance. The higher unoccupied DOS of the Pt 5d hole number stands for a stronger interaction between Pt NPs and support, which leads to an advanced electrocatalytic activity and durability. It can be concluded that the modification of carbon support by N-ALDTa<sub>2</sub>O<sub>5</sub> plays a significant role in affecting the electronic states of Pt NPs, thus forming the strong metal-support interaction and leading to the enhancement of catalytic activity and long-term stability of Pt NPs.

#### 4. Conclusion

In summary, we have successfully used the ALD method to prepare a novel Pt/N-ALDTa<sub>2</sub>O<sub>5</sub>/C electrocatalyst in which the carbon support is decorated by N-doped-Ta<sub>2</sub>O<sub>5</sub> particles and yields Pt NPs that are well-anchored and stick tightly on the modified carbon surface. Experimental results demonstrate that Pt/N-ALDTa<sub>2</sub>O<sub>5</sub>/C catalyst shows improved activity for the ORR compared to the Pt/C catalyst. More interestingly, the Pt/N-ALDTa<sub>2</sub>O<sub>5</sub>/C catalyst exhibits superior long-term durability, reflected by a mass activity two times higher than that of Pt/C, after 10,000 cycles of accelerated durability tests. The improved activity and stability are attributed to the introduction of a N-Ta<sub>2</sub>O<sub>5</sub> bridge layer between Pt NPs and carbon support, forming strong metal-support interactions and thus effectively prevent Pt nanocrystals from migration and aggregation. The X-ray absorption spectra suggests that the Pt/N-ALDTa<sub>2</sub>O<sub>5</sub>/C catalyst shows noticeable electron delocalization of Pt d orbitals and with electron transfer from Pt to N-Ta<sub>2</sub>O<sub>5</sub>/C support, which gives the most direct evidence for the strong interactions between Pt NPs and N-Ta<sub>2</sub>O<sub>5</sub>/C support. The result of this work provides insights for future design of electrocatalysts with high stability through increased interactions between catalytic metal particles and support.

#### Acknowledgments

This research was supported by Ballard Power Systems Inc., Natural Sciences and Engineering Research Council of Canada (NSERC), Canada Research Chair (CRC) Program, Canada Foundation for Innovation (CFI), Ontario Research Fund (ORF), Automotive Partnership of Canada, and the University of Western Ontario. Z. Song was supported by the Chinese Scholarship Council. Z. Song and M. Banis contributed equally to this work.

#### Appendix A. Supporting information

Supplementary data associated with this article can be found in the online version at [doi:10.1016/j.nanoen.2018.09.008](https://doi.org/10.1016/j.nanoen.2018.09.008).

#### References

- [1] M.K. Debe, *Nature* 486 (2012) 43.
- [2] T. Yoshida, K. Kojima, *Electrochim. Soc. Interface* 24 (2015) 45–49.

- [3] U. Eberle, B. Muller, R. von Helmolt, *Energy Environ. Sci.* 5 (2012) 8780–8798.
- [4] C.D. Young, Y.J. Mun, S. Yung-Eun, *Adv. Mater.* (2018) 1704123.
- [5] S. Park, Y. Shao, J. Liu, Y. Wang, *Energy Environ. Sci.* 5 (2012) 9331–9344.
- [6] L. Su, W. Jia, C.-M. Li, Y. Lei, *ChemSusChem* 7 (2014) 361–378.
- [7] S. Sui, X. Wang, X. Zhou, Y. Su, S. Riffat, C.-j. Liu, *J. Mater. Chem. A* 5 (2017) 1808–1825.
- [8] Z. Song, B. Wang, N. Cheng, L. Yang, D. Banham, R. Li, S. Ye, X. Sun, *J. Mater. Chem. A* 5 (2017) 9760–9767.
- [9] L. Guo, W.-J. Jiang, Y. Zhang, J.-S. Hu, Z.-D. Wei, L.-J. Wan, *ACS Catal.* 5 (2015) 2903–2909.
- [10] N. Cheng, M.N. Banis, J. Liu, A. Riese, X. Li, R. Li, S. Ye, S. Knights, X. Sun, *Adv. Mater.* 27 (2015) 277–281.
- [11] Y. Li, Y. Li, E. Zhu, T. McLouth, C.-Y. Chiu, X. Huang, Y. Huang, *J. Am. Chem. Soc.* 134 (2012) 12326–12329.
- [12] L. Li, L. Hu, J. Li, Z. Wei, *Nano Res.* 8 (2015) 418–440.
- [13] J.C. Meier, C. Galeano, I. Katsounaros, A.A. Topalov, A. Kostka, F. Schüth, K.J.J. Mayrhofer, *ACS Catal.* 2 (2012) 832–843.
- [14] J. Speder, A. Zana, I. Spanos, J.J.K. Kirkensgaard, K. Mortensen, M. Hanzlik, M. Arenz, *J. Power Sources* 261 (2014) 14–22.
- [15] N.G. Akalework, C.-J. Pan, W.-N. Su, J. Rick, M.-C. Tsai, J.-F. Lee, J.-M. Lin, L.-D. Tsai, B.-J. Hwang, *J. Mater. Chem.* 22 (2012) 20977–20985.
- [16] Z. Awaludin, M. Suzuki, J. Masud, T. Okajima, T. Ohsaka, *J. Phys. Chem. C* 115 (2011) 25557–25567.
- [17] M.N. Banis, S. Sun, X. Meng, Y. Zhang, Z. Wang, R. Li, M. Cai, T.-K. Sham, X. Sun, *J. Phys. Chem. C* 117 (2013) 15457–15467.
- [18] V.T.T. Ho, C.-J. Pan, J. Rick, W.-N. Su, B.-J. Hwang, *J. Am. Chem. Soc.* 133 (2011) 11716–11724.
- [19] S.-Y. Huang, P. Ganesan, S. Park, B.N. Popov, *J. Am. Chem. Soc.* 131 (2009) 13898–13899.
- [20] S.-Y. Huang, P. Ganesan, B.N. Popov, *ACS Catal.* 2 (2012) 825–831.
- [21] A. Kumar, V. Ramani, *ACS Catal.* 4 (2014) 1516–1525.
- [22] D. He, C. Zeng, C. Xu, N. Cheng, H. Li, S. Mu, M. Pan, *Langmuir* 27 (2011) 5582–5588.
- [23] N. Cheng, M.N. Banis, J. Liu, A. Riese, S. Mu, R. Li, T.-K. Sham, X. Sun, *Energy Environ. Sci.* 8 (2015) 1450–1455.
- [24] G.C. da Silva, M.R. Fernandes, E.A. Ticianelli, *ACS Catal.* (2018) 2081–2092.
- [25] A.D. Duma, Y.-C. Wu, W.-N. Su, C.-J. Pan, M.-C. Tsai, H.-M. Chen, J.-F. Lee, H.-S. Sheu, V.T.T. Ho, B.-J. Hwang, *ChemCatChem* (2018) 1–12.
- [26] R. Kou, Y. Shao, D. Mei, Z. Nie, D. Wang, C. Wang, V.V. Viswanathan, S. Park, I.A. Aksay, Y. Lin, Y. Wang, J. Liu, *J. Am. Chem. Soc.* 133 (2011) 2541–2547.
- [27] T. Binninger, E. Fabbri, R. Kötz, T.J. Schmidt, *J. Electrochem. Soc.* 161 (2014) 121–128.
- [28] A. Lewera, L. Timperman, A. Roguska, N. Alonso-Vante, *J. Phys. Chem. C* 115 (2011) 20153–20159.
- [29] A. Epshteyn, Y. Garsany, K.L. More, H.M. Meyer, V. Jain, A.P. Purdy, K.E. Swider-Lyons, *ACS Catal.* 5 (2015) 3662–3674.
- [30] Y. Garsany, M.B. Sassin, B.D. Gould, K. Swider-Lyons, *ECS Trans.* 69 (2015) 1243–1250.
- [31] A. Korovina, Y. Garsany, A. Epshteyn, A.P. Purdy, K. More, K.E. Swider-Lyons, D.E. Ramaker, *J. Phys. Chem. C* 116 (2012) 18175–18183.
- [32] J. Seo, D. Cha, K. Takanebe, J. Kubota, K. Domen, *ACS Catal.* 3 (2013) 2181–2189.
- [33] J. Seo, L. Zhao, D. Cha, K. Takanebe, M. Katayama, J. Kubota, K. Domen, *J. Phys. Chem. C* 117 (2013) 11635–11646.
- [34] C.W.B. Bezerra, L. Zhang, H. Liu, K. Lee, A.L.B. Marques, E.P. Marques, H. Wang, J. Zhang, *J. Power Sources* 173 (2007) 891–908.
- [35] A. Ishihara, M. Tamura, K. Matsuzawa, S. Mitsushima, K.-i. Ota, *Electrochim. Acta* 55 (2010) 7581–7589.
- [36] T. Oh, J.Y. Kim, Y. Shin, M. Engelhard, K.S. Weil, *J. Power Sources* 196 (2011) 6099–6103.
- [37] J. Liu, X. Sun, *Nanotechnol* 26 (2015) 024001.
- [38] X. Meng, Q. Yang, X. Sun, *Adv. Mater.* 24 (2012) 3589–3615.
- [39] N. Cheng, Y. Shao, J. Liu, X. Sun, *Nano Energy* 29 (2016) 220–242.
- [40] X. Li, X. Meng, J. Liu, D. Geng, Y. Zhang, M.N. Banis, Y. Li, J. Yang, R. Li, X. Sun, *Adv. Funct. Mater.* 22 (2012) 1647–1654.
- [41] J. Liu, M.N. Banis, X. Li, A. Lushington, M. Cai, R. Li, T.-K. Sham, X. Sun, *J. Phys. Chem. C* 117 (2013) 20260–20267.
- [42] X. Meng, J. Liu, X. Li, M.N. Banis, J. Yang, R. Li, X. Sun, *RSC Adv.* 3 (2013) 7285–7288.
- [43] J. Liu, X. Meng, Y. Hu, D. Geng, M.N. Banis, M. Cai, R. Li, X. Sun, *Carbon* 52 (2013) 74–82.
- [44] A. Mansour, J. Cook Jr, D. Sayers, *J. Phys. Chem.* 88 (1984) 2330–2334.
- [45] T. Sham, S. Naftel, I. Coulthard, *J. Appl. Phys.* 79 (1996) 7134–7138.
- [46] M. Kuhn, T. Sham, *Phys. Rev. B* 49 (1994) 1647.
- [47] S. Sun, G. Zhang, N. Gauquelin, N. Chen, J. Zhou, S. Yang, W. Chen, X. Meng, D. Geng, M.N. Banis, R. Li, S. Ye, S. Knights, G.A. Botton, T.-K. Sham, X. Sun, *Sci. Rep.* 3 (2013) 1775.
- [48] N. Cheng, S. Stambula, D. Wang, M.N. Banis, J. Liu, A. Riese, B. Xiao, R. Li, T.-K. Sham, L.-M. Liu, *Nat. Commun.* 7 (2016) 13638.
- [49] S. Trasatti, O. Petrii, *Pure Appl. Chem.* 63 (1991) 711–734.
- [50] M. Zhang, P. Hou, Z. Wang, P. Kang, *ChemElectroChem* 5 (2018) 799–804.
- [51] K. Mayrhofer, D. Strmcnik, B. Blizanac, V. Stamenkovic, M. Arenz, N. Markovic, *Electrochim. Acta* 53 (2008) 3181–3188.



**Zhongxin Song** is currently a Ph.D. candidate in Prof. Xueliang (Andy) Sun's Group at the University of Western Ontario, Canada. She received her B.S. degree and M.S. degree in Polymer Science and Engineering from Qingdao University of Science and Technology (China) in 2011 and 2014, respectively. Her current research interests focus on design and synthesis of metal nanomaterials, single atom catalyst, and MOFs materials for fuel cells application.



**Dr. Dustin Banham** graduated with a first class honors degree in Chemical Physics, and a Ph.D. in electrochemistry from the University of Calgary under the supervision of Dr. Viola Birss. His Ph.D. thesis was focused on design of porous carbon materials for electrochemical applications, and was performed in collaboration with Ballard. He joined Ballard in 2012 as a postdoc, and in 2013 he became a full time Research Scientist. In 2015 he was promoted to Senior Research Scientist. He has 10 years of experience in PEMFC catalyst research. Currently, his work at Ballard is focused on advanced electrocatalyst and catalyst layer development.



**Dr. Mohammad Norouzi Banis** is a research engineer in Prof. Xueliang (Andy) Sun's group at the University of Western Ontario, Canada. He received his Ph.D. degree in 2013 in Materials Science and Engineering from Western University, on the study of nanostructured low temperature fuel cells and application of x-ray absorption spectroscopy in energy related systems. His current research interests include study of metal ion, metal air and nanocatalysts via in-situ synchrotron-based techniques.



**Yang Zhao** is currently a Ph.D. candidate in Prof. Xueliang (Andy) Sun's Group at the University of Western Ontario, Canada. He received his B.S. degree and M.S. degree in Chemical Engineering and Technology from Northwestern Polytechnical University (Xi'an, China) in 2011 and 2014, respectively. His current research interests focus on atomic layer deposition in the application of lithium/sodium ion batteries and all-solid-state batteries.



**Dr. Lei Zhang** received his BS degree in Chemistry (2008) and Ph.D. degree in Nanomaterial Chemistry (2014) from Xiamen University with Prof. Zhaoxiong Xie. He was a visiting graduate student at Georgia Institute of Technology in Prof. Younan Xia's group from 2012 to 2014. From 2015–2016, he worked as a Postdoc at Collaborative Innovation Center of Chemical Science and Engineering in Tianjin University. He is currently a postdoctoral associate with Prof. Xueliang Sun at Western University. His research interests include the design and synthesis of metal nanomaterials and single atom catalysts for fuel cells, carbon dioxide reduction, and water splitting devices.



**Jianneng Liang** is currently a Ph.D. candidate in the department of Mechanical and Materials Engineering at the University of Western Ontario, Canada. He got his B.S. in metallurgical engineering in 2015 from Central South University, China. Currently, his research interests include solid-state polymer electrolytes, hybrid electrolyte, all-solid-state LIBs and Li-S batteries, and the interfacial study in all-solid-state batteries.



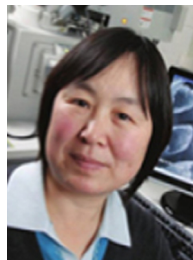
**Dr. Biqiong Wang** is a Research Scientist at General Motors. She received her Ph.D. degree in 2017 in Prof. Xueliang (Andy) Sun's Nanomaterials and Energy Group at Western University, Canada. She received her Bachelor's degree in Materials Science in 2012 at the City University of Hong Kong. Her research interests are associated with the application of atomic layer deposition in all-solid-state batteries. She is also co-supervised by Prof. T. K. Sham from Chemistry Department in Western University. Part of her work is related to the study of energy materials via synchrotron radiation.



**Matthew Zheng** is currently an undergraduate engineering student at the University of British Columbia (UBC). He was a visiting student for the summer at the University of Western Ontario (UWO) in 2017 and 2018. His research focuses on the application of 3D printing techniques in LIB design with a particular focus on solid state LIBs.



**Dr. Lijun Yang** is a Research Scientist at Ballard Power Systems. She earned her Ph.D. from a joint program between South China University of Technology and Brookhaven National Laboratory. She was a postdoctoral fellow at Institut national de la recherche scientifique (EMT) at Montreal, Canada. She joined Ballard in 2015 as postdoc and became full timer two years later. She has 10 years of experience in PEMFC catalyst research. Her current work is focus on the application of advanced electro-catalysts in the catalyst layers for PEM fuel cell.



**Ruying Li** is a research engineer at Prof. Xueliang (Andy) Sun's Nanomaterial and Energy Group at the University of Western Ontario, Canada. She received her Master degree in Material Chemistry under the supervision of Prof. George Thompson in 1999 at University of Manchester, UK, followed by work as a research assistant under the direction of Prof. Keith Mitchell at the University of British Columbia and under the direction of Prof. Jean-Pol Dodelet at l'Institut national de la recherche scientifique (INRS), Canada. Her current research interests are associated with synthesis and characterization of nanomaterials for electrochemical energy storage and conversion.



**Dr. Siyu Ye** is a Fellow of Canadian Academy of Engineering and Principal Research Scientist at Ballard Power Systems. He is also an Adjunct Professor at the University of British Columbia, University of Waterloo, South China University of Technology, and South University of Science and Technology of China. He earned his Ph.D. from Xiamen University. He was a Postdoctoral Fellow at the University Duisburg and University of Quebec at Montreal. He has more than twenty years of fuel cell experience with expertise in electrocatalysis and MEA design. He has over 100 peer-reviewed papers, and over 50 patents and patent applications.



**Prof. Xueliang Sun** is a Canada Research Chair in Development of Nanomaterials for Clean Energy, Fellow of the Royal Society of Canada and Canadian Academy of Engineering and Full Professor at the University of Western Ontario, Canada. Dr. Sun received his Ph.D. in materials chemistry in 1999 from the University of Manchester, UK, which he followed up by working as a postdoctoral fellow at the University of British Columbia, Canada and as a Research Associate at L'Institut National de la Recherche Scientifique (INRS), Canada. His current research interests are focused on advanced materials for electrochemical energy storage and conversion, including electrocatalysis in fuel cells and electrodes in lithium-ion batteries and metal-air battery.